

## Research Article

Jianlin Xu\*, Jinqiang Zhao, Chenghu Kang, Lei Niu, Jianbin Zhang, Jiqiang Ma, and Chunyan Ju

# Synthesis and mechanical properties of nano-Sb<sub>2</sub>O<sub>3</sub>/BPS-PP composites

<https://doi.org/10.1515/secm-2020-0014>

Received Nov 14, 2019; accepted Mar 25, 2020

**Abstract:** In view of the limitation of wide application of polypropylene (PP) with low strength, poor low-temperature brittleness and easy combustion, a kind of PP matrix nanocomposites was designed and prepared. Sb<sub>2</sub>O<sub>3</sub> nanoparticles (nano-Sb<sub>2</sub>O<sub>3</sub>) modified by silane coupling agent of KH550 were dispersed into brominated polystyrene (BPS)-PP matrix by ball milling dispersion and melt blending method, respectively. And the nano-Sb<sub>2</sub>O<sub>3</sub>/BPS-PP composites samples were obtained by injection molding method. The effects of nano-Sb<sub>2</sub>O<sub>3</sub> particles on mechanical properties of nano-Sb<sub>2</sub>O<sub>3</sub>/BPS-PP composites were investigated. The results showed that the surface of nano-Sb<sub>2</sub>O<sub>3</sub> particles was successfully modified by the KH550 and the interfacial adhesion between nano-Sb<sub>2</sub>O<sub>3</sub> and PP matrix was improved. With increasing of the mass fraction of nano-Sb<sub>2</sub>O<sub>3</sub>, the tensile strength and impact strength of nano-Sb<sub>2</sub>O<sub>3</sub>/BPS-PP composites were improved accompanying by increasing of crystallinity and refining grain of the composites. When the mass fraction of nano-Sb<sub>2</sub>O<sub>3</sub> was 3 wt%, the tensile strength of nano-Sb<sub>2</sub>O<sub>3</sub>/BPS-PP composites was 43 MPa, which was 30.3% higher than that of PP. When the mass fraction of nano-Sb<sub>2</sub>O<sub>3</sub> was 2 wt%, the impact strength of the composites was 44.19 kJ·m<sup>-2</sup>, which was 30.8% higher than that of PP.

**Keywords:** polypropylene; composites; Sb<sub>2</sub>O<sub>3</sub> nanoparticle; mechanical properties; crystallinity

## 1 Introduction

Polypropylene (PP) is an important engineering plastic. It has been widely used in many engineering fields because of its some advantages, such as good mechanical properties, corrosion resistance, easy formability, etc [1, 2]. However, PP also has some disadvantages, such as low strength, poor low-temperature brittleness, easy combustion, etc [3]. In order to improve the comprehensive properties of PP, it is an effective method that some nanoparticles are filled into PP matrix. Nano-composites have excellent mechanical properties because nanoparticles have some characteristics of surface effect, volume effect and quantum size effect, especially nanoparticles have good interface combination ability with polymer matrix [4, 5]. However, the particle size, shape and surface structure of nanoparticles have significant influences on the distribution of the nanoparticles in the matrix and the interfacial compatibility between the nanoparticles and the matrix. When the mass fraction of nanoparticles is too high, the nanoparticles easily form aggregates in the matrix, thus deteriorating the mechanical properties of nano-composites [6]. Therefore, the preparation of nano-composites with excellent comprehensive properties has become an important target for material researches.

Sb<sub>2</sub>O<sub>3</sub> nanoparticle (nano-Sb<sub>2</sub>O<sub>3</sub>) is a new kind of synergistic flame retardant, which can reduce the amount of halogen flame-retardants in the synergistic systems of nano-Sb<sub>2</sub>O<sub>3</sub> and halogen flame-retardants. Nano-composites can obtain excellent flame retardancy based on adding nano-Sb<sub>2</sub>O<sub>3</sub> [7]. We added nano-Sb<sub>2</sub>O<sub>3</sub> into PP matrix and found that nano-Sb<sub>2</sub>O<sub>3</sub> could improve the flame retardancy of PP matrix composites [8]. Sb<sub>2</sub>O<sub>3</sub> as nanoparticles in PP matrix has a positive effect on the mechanical properties of the matrix [9]. In order to thoroughly study the effects of nano-Sb<sub>2</sub>O<sub>3</sub> on the mechanical properties of polymer matrix composites, nano-Sb<sub>2</sub>O<sub>3</sub>/BPS-PP composites were prepared in the paper, and then the ef-

**\*Corresponding Author: Jianlin Xu:** State Key Laboratory of Advanced Processing and Recycling of Non-ferrous Metals, Lanzhou University of Technology, Lanzhou 730050, China; and Baiyin Research Institute of Novel Materials, Lanzhou University of Technology, Baiyin 730900, China; Email:ggdjlxx@sina.com

**Jinqiang Zhao, Chenghu Kang, Lei Niu, Jianbin Zhang:** State Key Laboratory of Advanced Processing and Recycling of Non-ferrous Metals, Lanzhou University of Technology, Lanzhou 730050, China; and Baiyin Research Institute of Novel Materials, Lanzhou University of Technology, Baiyin 730900, China

**Jiqiang Ma:** State Key Laboratory of Advanced Processing and Recycling of Non-ferrous Metals, Lanzhou University of Technology, Lanzhou 730050, China

**Chunyan Ju:** School of Materials and Chemical Engineering, College of Technology and Engineering. LUT, Lanzhou, 730300, China

ffects of nano-Sb<sub>2</sub>O<sub>3</sub> on the mechanical properties of nano-Sb<sub>2</sub>O<sub>3</sub>/BPS-PP composites were studied.

## 2 Experimental

### 2.1 Materials

The surface modifier was silane coupling agent KH-550 (Qufu Yishun Chemical Co., Ltd., China). The matrix material was homopolymer PP (Sinopec Beijing Yanshan Company, China) with molecular weight of 300000 and melting index of 1 g/10 min. Nano-Sb<sub>2</sub>O<sub>3</sub> with an average particle size of 50~100 nm were prepared by our research group using high-energy ball milling method. The flame retardants were brominated polystyrene (BPS) with molecular weight more than 200000 (Dow Chemical Company, U.S.A.).

### 2.2 Preparation of the experimental materials

Nano-Sb<sub>2</sub>O<sub>3</sub> particles were prepared by QM-3SP04 planetary ball mill (Nanjing Laibu Science and Technology Industry Co., Ltd., China). In order to investigate the effects of nano-Sb<sub>2</sub>O<sub>3</sub> particles with different surface states on the mechanical properties of the experimental composites, modified and unmodified nanoparticles were used as reinforcing particles, respectively. Modified nano-Sb<sub>2</sub>O<sub>3</sub> particles were modified by KH-550 in the preparation processing and labeled as m-nano-Sb<sub>2</sub>O<sub>3</sub>. Unmodified nano-Sb<sub>2</sub>O<sub>3</sub> particles were labeled as um-nano-Sb<sub>2</sub>O<sub>3</sub>. Nano-Sb<sub>2</sub>O<sub>3</sub> with a certain mass fraction was mixed with BPS and PP matrix by ball milling method to obtain uniformly dispersing composite powders. The compositions of the experimental materials are shown in Table 1. The composite powders were extruded by SJZS-10A twin-screw extruders (Wuhan Ruiming Machinery Manufacture Co., Ltd., China)

to obtain nano-Sb<sub>2</sub>O<sub>3</sub>/BPS-PP composites, and then the experimental samples were prepared by SZS-20 injection molding machine (Wuhan Ruiming Machinery Manufacture Co., Ltd., China).

### 2.3 Measurements and characterizations

The surface modification state of nano-Sb<sub>2</sub>O<sub>3</sub> was analyzed by Fourier transform infrared spectrometer (FT-IR, Thermo Nicolet Corporation, U.S.A.). The morphology and dispersibility of nano-Sb<sub>2</sub>O<sub>3</sub> were observed by JEM-2010 transmission electron microscope (TEM, JEOL Ltd., Japan). The effects of nano-Sb<sub>2</sub>O<sub>3</sub> on the crystallization properties of nano-Sb<sub>2</sub>O<sub>3</sub>/BPS-PP composites were analyzed by TG/DTA-1 differential scanning calorimeter tester (DSC, Perkin-Elmer Ltd., U.S.A.). In the DSC testing process, the samples were quickly heated to 200°C and kept temperature for 5 minutes to eliminate thermal history. Then the samples were cooled to 50°C at a cooling rate of 10°C/min, and kept temperature for 5 minutes. Finally the temperature was raised to 200°C at a heating rate of 10°C/min. The cooling and the second heating curves were recorded. The tensile strength and Young's modulus of the specimens were tested by HS-100KN universal mechanical tensile testing machine (Yangzhou Huahui Inspection Instrument Co., Ltd., China). The tensile testing was carried out according to GB/T 1040-2006 of Chinese National Standards. The notched impact strength of specimens was tested by XJU-22 impact test machine (Jinan Naier Co., Ltd., China). The impact test was carried out according to GB/T 1843-2008 of Chinese National Standards. The number of each group of mechanical properties testing specimens was 5, and the testing value took an average value. The fracture surfaces of tensile specimens and impact specimens were observed by scanning electron microscope (SEM, Thermo Nicolet Corporation, U.S.A.).

## 3 Results and discussion

### 3.1 Surface modification analysis of nano-Sb<sub>2</sub>O<sub>3</sub>

The FT-IR spectra of nano-Sb<sub>2</sub>O<sub>3</sub> and the experimental materials are presented in Figure 1. In the curve (a) of um-nano-Sb<sub>2</sub>O<sub>3</sub> particles, the peaks located at 3438cm<sup>-1</sup> and 1626cm<sup>-1</sup> correspond to the stretching vibration characteristic and bending vibration characteristic of hydroxyl, respectively. It shows that the surface of the unmodi-

**Table 1:** The compositions of the experimental materials (mass fraction)

Sample No.	Sb <sub>2</sub> O <sub>3</sub> /wt%	BPS/wt%	PP/wt%
1	0	0	100
2	1	8	91
3	2	8	90
4	3	8	89
5	4	8	88
6	5	8	87

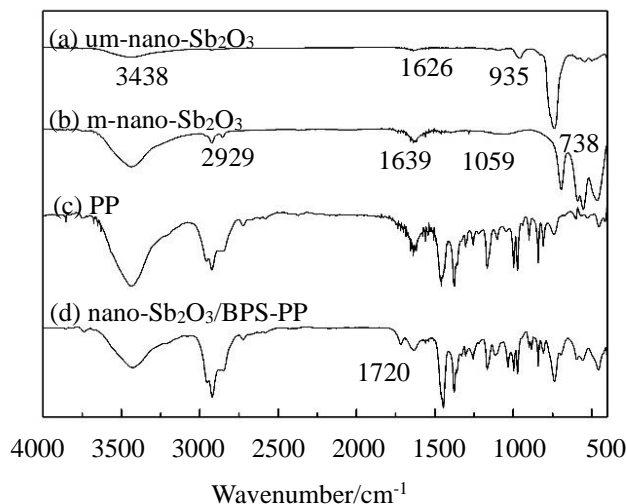


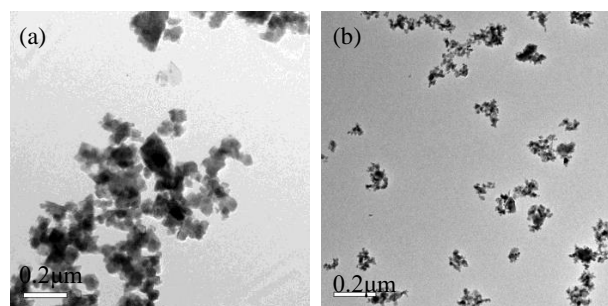
**Figure 1:** FT-IR spectra of nano-Sb<sub>2</sub>O<sub>3</sub> and the experimental materials

fied nano-Sb<sub>2</sub>O<sub>3</sub> particles contains hydroxyl because the nanoparticles easily absorbed moisture in the air attributed to the smaller particle size, higher specific surface area and surface energy of the nanoparticles. The curve (b) is the FT-IR spectrum of m-nano-Sb<sub>2</sub>O<sub>3</sub> particles modified by KH550. The intensity of stretching vibration characteristic peak of hydroxyl at 3438 cm<sup>-1</sup> increases and the bending vibration characteristic peak of hydroxyl at 1626 cm<sup>-1</sup> disappears. At the same time, some new peaks are observed in the curve (b). The peak at 1639 cm<sup>-1</sup> is assigned to N-H bending vibration peak. The peak at 1059 cm<sup>-1</sup> is due to the stretching mode of C-O-C, and the peaks near 2929 cm<sup>-1</sup> are associated with -CH<sub>3</sub> and -CH<sub>2</sub>- vibrations. These new peaks belong to the typical characteristics of KH550, indicating that Sb<sub>2</sub>O<sub>3</sub> nanoparticles are successfully modified by KH550. When the surface of nano-Sb<sub>2</sub>O<sub>3</sub> adsorbs KH550, the hydroxyl groups on the surface of nano-Sb<sub>2</sub>O<sub>3</sub> can condense with R-Si-OH of the hydrolysate of KH550. The condensation can change the bond energy and bond length of nano-Sb<sub>2</sub>O<sub>3</sub> particles surfaces, which leads to the shift of the absorption peak near 738 cm<sup>-1</sup> toward lower wave numbers.

The curve (c) and (d) in Figure 1 are FT-IR spectra of PP and the modified nano-Sb<sub>2</sub>O<sub>3</sub>/BPS-PP composites, respectively. It can be seen that the characteristic absorption peak of the nano-Sb<sub>2</sub>O<sub>3</sub>/BPS-PP composites containing modified nano-Sb<sub>2</sub>O<sub>3</sub> particles has some changes compared with those of PP. For example, the intensity of the characteristic absorption peak at 2929 cm<sup>-1</sup> obviously increases, which indicates that the numbers of -CH<sub>3</sub> and -CH<sub>2</sub>- groups in the nano-Sb<sub>2</sub>O<sub>3</sub>/BPS-PP composites increases due to KH550 coating on the surface of the nano-

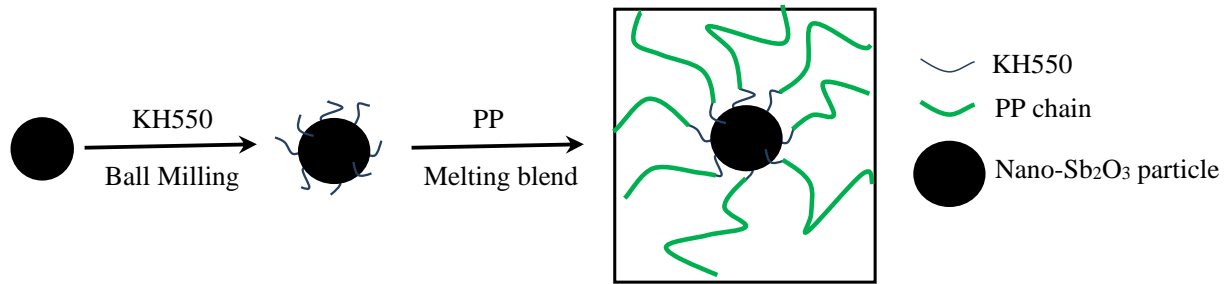
Sb<sub>2</sub>O<sub>3</sub> particles. And a new characteristic absorption peak of C=O bond at 1720 cm<sup>-1</sup> of the nano-Sb<sub>2</sub>O<sub>3</sub>/BPS-PP composites appears because C-O-C group of KH550 coating on surface of nano-Sb<sub>2</sub>O<sub>3</sub> particles reacts with -CH<sub>3</sub> group in PP to form C=O bond.

Figure 2 shows TEM micrographs of unmodified and modified nano-Sb<sub>2</sub>O<sub>3</sub> particles, respectively. It can be seen from Figure 2 (a) that there are obvious agglomeration phenomena of unmodified nano-Sb<sub>2</sub>O<sub>3</sub> particles and the size of aggregate is higher than 200 nm. These aggregates presents as a loose state and the particles clusters are not compact. Figure 2 (b) shows that nano-Sb<sub>2</sub>O<sub>3</sub> particles modified by KH550 disperse uniformly, which indicates that the dispersibility of nano-Sb<sub>2</sub>O<sub>3</sub> particles in the composites is significantly improved due to the surface modification of nano-Sb<sub>2</sub>O<sub>3</sub> particles. Surface modification of nanoparticles is also well-known as an effective way to improve the dispersion of nanoparticles in polymer matrix [10].



**Figure 2:** TEM micrographs of nano-Sb<sub>2</sub>O<sub>3</sub> particles (a) um-nano-Sb<sub>2</sub>O<sub>3</sub> particles; (b) m-nano-Sb<sub>2</sub>O<sub>3</sub> particles

Figure 3 shows the schematic diagram of modification mechanism of nano-Sb<sub>2</sub>O<sub>3</sub> particles modified by KH550 and the interfacial microstructure between nano-Sb<sub>2</sub>O<sub>3</sub> particles and PP matrix. A modified layer with reactive functional groups is formed on the surface of the modified nano-Sb<sub>2</sub>O<sub>3</sub> due to the existence of KH550. These reactive functional groups are mainly C-O-C, -CH<sub>2</sub>- and partial -O-H groups of KH550. The surface of nano-Sb<sub>2</sub>O<sub>3</sub> particles coated by these groups exhibits hydrophobicity property. Therefore, the modified nano-Sb<sub>2</sub>O<sub>3</sub> particles have good wettability to polymer matrix and can improve the dispersibility of nano-Sb<sub>2</sub>O<sub>3</sub> particles in PP matrix. When nano-Sb<sub>2</sub>O<sub>3</sub> particles are blended into PP matrix by means of melt blending method, the C-O-C group of the surface modified layer of nano-Sb<sub>2</sub>O<sub>3</sub> particles can react with -CH<sub>3</sub> group of PP chains at high temperature to form a interfacial microstructure basing on C=O covalent bond and hy-



**Figure 3:** The schematic diagram of modification mechanism of nano-Sb<sub>2</sub>O<sub>3</sub> particles modified by KH550 and interfacial microstructure between nano-Sb<sub>2</sub>O<sub>3</sub> particles and PP matrix

**Table 2:** The mechanical properties of PP and nano-Sb<sub>2</sub>O<sub>3</sub>/BPS-PP composites

Sample No.	Young's modulus/GPa	standard error	Tensile strength/MPa	standard error	Static fracture toughness/(MJ·m <sup>-3</sup> )	standard error
1	0.852	0.06	33	1.91	0.979	0.05
2	1.076	0.05	38	1.54	1.225	0.06
3	1.156	0.06	40	1.57	1.628	0.04
4	1.259	0.07	43	1.77	1.573	0.05
5	1.125	0.06	40	1.69	1.494	0.06
6	1.048	0.05	37	1.81	1.367	0.05

drogen bond. It is a transition interfacial microstructure of nano-Sb<sub>2</sub>O<sub>3</sub> particle-KH550-PP matrix, resulting in obtaining better interfacial bonding strength between nano-Sb<sub>2</sub>O<sub>3</sub> particles and PP matrix.

### 3.2 Mechanical properties of nano-Sb<sub>2</sub>O<sub>3</sub>/BPS-PP composites

#### 3.2.1 Tensile properties of nano-Sb<sub>2</sub>O<sub>3</sub>/BPS-PP composites

The tensile strength, Young's modulus and static fracture toughness of PP and nano-Sb<sub>2</sub>O<sub>3</sub>/BPS-PP composites with different mass fraction of modified nano-Sb<sub>2</sub>O<sub>3</sub> particles are shown in Table 2. When the mass fraction of nano-Sb<sub>2</sub>O<sub>3</sub> particle is less than 3 wt%, the tensile strength and Young's modulus of nano-Sb<sub>2</sub>O<sub>3</sub>/BPS-PP composites increase in different degrees with increasing of the mass fraction of nano-Sb<sub>2</sub>O<sub>3</sub> particle. The nano-Sb<sub>2</sub>O<sub>3</sub> particles with lower mass fraction can be uniformly dispersed in PP matrix. When the experimental material is subjected to external force, the nano-Sb<sub>2</sub>O<sub>3</sub> particles can bear the partial load transferred by PP matrix, thus improve the tensile strength and deformation resistance of the nano-Sb<sub>2</sub>O<sub>3</sub>/BPS-PP composites. When the mass fraction of nano-Sb<sub>2</sub>O<sub>3</sub> particles is 2 wt%, the tensile strength of

nano-Sb<sub>2</sub>O<sub>3</sub>/BPS-PP composites is 40 MPa, which is 21.2% higher than that of PP. When the mass fraction of nano-Sb<sub>2</sub>O<sub>3</sub> particles is 3 wt%, the tensile strength of nano-Sb<sub>2</sub>O<sub>3</sub>/BPS-PP composites reaches the maximum value of 43 MPa, which is 30.3% higher than that of PP. Unfortunately, the static fracture toughness of the composites decreases because nano-Sb<sub>2</sub>O<sub>3</sub> particles begin to agglomerate in PP matrix. The influence of the aggregates on the tensile strength of the composites is relatively smaller due to the small amount of agglomeration [11]. Therefore, the tensile strength of nano-Sb<sub>2</sub>O<sub>3</sub>/BPS-PP composites is not significantly affected negatively. When the mass fraction of nano-Sb<sub>2</sub>O<sub>3</sub> particles is more than 3 wt%, the tensile strength and static fracture toughness of nano-Sb<sub>2</sub>O<sub>3</sub>/BPS-PP composites decrease because nano-Sb<sub>2</sub>O<sub>3</sub> particles gradually aggregate in PP matrix and form some large aggregates. These aggregates can easily separate from PP matrix due to their large volume and then form large crack in the matrix when the nano-Sb<sub>2</sub>O<sub>3</sub>/BPS-PP composites are subjected to external force, which leads to sharply decrease on the tensile strength and static fracture toughness of the composites.

Figure 4 shows the relationship between tensile strength of the experimental nano-Sb<sub>2</sub>O<sub>3</sub>/BPS-PP composites and the mass fraction of unmodified and modified nano-Sb<sub>2</sub>O<sub>3</sub> particles, respectively. With increasing of the mass fraction of nano-Sb<sub>2</sub>O<sub>3</sub> particles, the tensile strength



of nano-Sb<sub>2</sub>O<sub>3</sub>/BPS-PP composites firstly increases and then decreases. The tensile strength of the modified nano-Sb<sub>2</sub>O<sub>3</sub>/BPS-PP composites is significantly higher than that of the unmodified nano-Sb<sub>2</sub>O<sub>3</sub>/BPS-PP composites containing the same mass fraction of the nano-Sb<sub>2</sub>O<sub>3</sub> particles. When the mass fraction of the unmodified nano-Sb<sub>2</sub>O<sub>3</sub> particles is 3 wt%, the tensile strength of the unmodified nano-Sb<sub>2</sub>O<sub>3</sub>/BPS-PP composites reaches the maximum value of 38 MPa, which is 15.2% higher than that of PP. If the modified nano-Sb<sub>2</sub>O<sub>3</sub> particles with 3 wt% of the mass fraction are used, the tensile strength of the nano-Sb<sub>2</sub>O<sub>3</sub>/BPS-PP composites reaches the maximum of 43 MPa, which is 30.3% higher than that of PP and 13.2% higher than that of unmodified nano-Sb<sub>2</sub>O<sub>3</sub>/BPS-PP composites with the same mass fraction of the unmodified nano-Sb<sub>2</sub>O<sub>3</sub> particles. The nano-Sb<sub>2</sub>O<sub>3</sub> particles modified by KH550 can obviously improve the interfacial bonding properties between nano-Sb<sub>2</sub>O<sub>3</sub> particles and PP matrix. Due to the better interface compatibility between the nano-Sb<sub>2</sub>O<sub>3</sub> particles and PP matrix, nano-Sb<sub>2</sub>O<sub>3</sub> particles can not easy to fall off from PP matrix and eliminate local stress under external force. Therefore, tensile strength of the composites is increased.

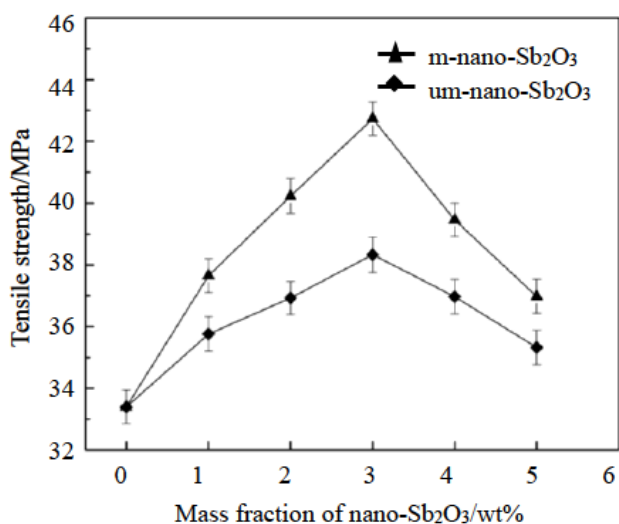


**Figure 4:** Relationship between tensile strength of the experimental materials and mass fraction of nano-Sb<sub>2</sub>O<sub>3</sub> particles

### 3.2.2 Impact strength of nano-Sb<sub>2</sub>O<sub>3</sub>/BPS-PP composites

Figure 5 shows the relationship between impact strength of the experimental nano-Sb<sub>2</sub>O<sub>3</sub>/BPS-PP composites and

mass fraction of unmodified and modified nano-Sb<sub>2</sub>O<sub>3</sub> particles, respectively. It can be seen from Figure 5 that the impact strength of nano-Sb<sub>2</sub>O<sub>3</sub>/BPS-PP composites increases firstly and then decreases with increasing of the mass fraction of nano-Sb<sub>2</sub>O<sub>3</sub> particles. For the unmodified nano-Sb<sub>2</sub>O<sub>3</sub> particles, the impact strength of the nano-Sb<sub>2</sub>O<sub>3</sub>/BPS-PP composites containing um-nano-Sb<sub>2</sub>O<sub>3</sub> particles with 2 wt% of mass fraction reaches the maximum value of 38.98 kJ·m<sup>-2</sup>, which is 15.35% higher than that of PP. For the modified nano-Sb<sub>2</sub>O<sub>3</sub> particles, it can effectively improve the impact strength of the nano-Sb<sub>2</sub>O<sub>3</sub>/BPS-PP composites. When the mass fraction of m-nano-Sb<sub>2</sub>O<sub>3</sub> particles is 2 wt%, the impact strength of the composites has the maximum value of 44.19 kJ·m<sup>-2</sup>, which is 30.77% higher than that of PP and 13.62% higher than that of nano-Sb<sub>2</sub>O<sub>3</sub>/BPS-PP composites containing um-nano-Sb<sub>2</sub>O<sub>3</sub> particles with 2 wt% of mass fraction.

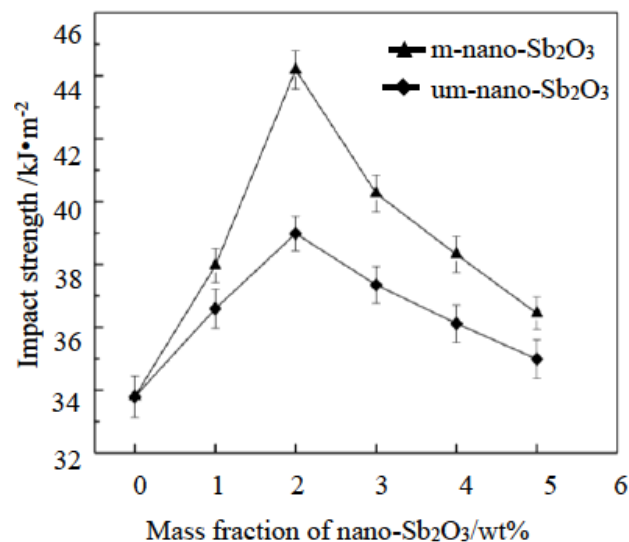


**Figure 5:** Relationship between impact strength of the experimental materials and mass fraction of nano-Sb<sub>2</sub>O<sub>3</sub> particles

Figure 6 shows the impact fracture SEM images of the nano-Sb<sub>2</sub>O<sub>3</sub>/BPS-PP composites with different mass fractions of nano-Sb<sub>2</sub>O<sub>3</sub> particles. It can be seen from Figure 6 (a) and (b) that the impact fracture surfaces of the nano-Sb<sub>2</sub>O<sub>3</sub>/BPS-PP composites are smoother when the mass fraction of nano-Sb<sub>2</sub>O<sub>3</sub> particles is less than 3 wt%. There are some regular water ripple lines on the fracture surface. The impact strength of the composites is lower. It can be seen from Figure 6 (c) that the amount of water ripple lines on the fracture surface of nano-Sb<sub>2</sub>O<sub>3</sub>/BPS-PP composites containing nano-Sb<sub>2</sub>O<sub>3</sub> particles with 3 wt% of mass fraction is less. Meanwhile, there are some smaller aggregates of Sb<sub>2</sub>O<sub>3</sub> particles. These aggregates are tightly wrapped in

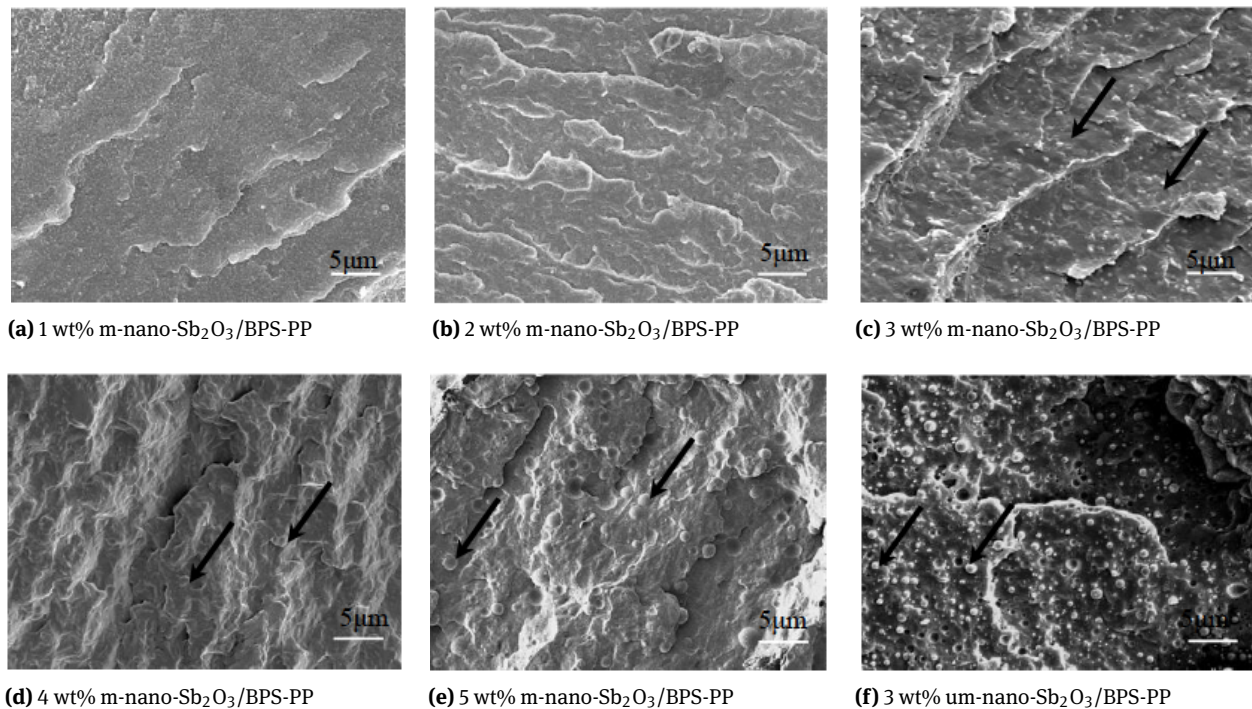


**Figure 6:** Impact fracture SEM images of the experimental nano-Sb<sub>2</sub>O<sub>3</sub>/BPS-PP composites

PP matrix to form compact microstructure of the composites. Therefore, the interface compatibility between nano-Sb<sub>2</sub>O<sub>3</sub> particles and PP matrix is better. As shown in Figure 6 (d) and (e), the impact fracture surfaces of the experimental nano-Sb<sub>2</sub>O<sub>3</sub>/BPS-PP composites are rougher and show the brittle fracture. The fracture surface has some uneven distribution aggregates of Sb<sub>2</sub>O<sub>3</sub> particles, and the size of aggregates becomes larger. There are some larger gaps between the aggregates and PP matrix, which indicates that the interfacial compatibility between the Sb<sub>2</sub>O<sub>3</sub> particles and PP matrix becomes worse. The nano-Sb<sub>2</sub>O<sub>3</sub> particles with less than 3 wt% of mass fraction can be uniformly dispersed in PP matrix. When the nano-Sb<sub>2</sub>O<sub>3</sub>/BPS-PP composites is impacted, the Sb<sub>2</sub>O<sub>3</sub> particles dispersed uniformly in PP matrix can absorb a part of the energy as the stress concentration point accompanying with that the PP matrix also takes place yield to produce plastic deformation and absorbs large amount of impact energy [12]. Meanwhile, these rigid Sb<sub>2</sub>O<sub>3</sub> particles can also prevent the crack forming and promote the cracks tip passivation in cracks growth process, resulting in increasing the crack growth energy and preventing the destructive fracture of the composites by mean of the crack growth. Therefore, the impact strength of nano-Sb<sub>2</sub>O<sub>3</sub>/BPS-PP composites increases with increasing of the mass fraction of nano-Sb<sub>2</sub>O<sub>3</sub> particles when the mass fraction of nano-Sb<sub>2</sub>O<sub>3</sub>

particles is lower. When the mass fraction of nano-Sb<sub>2</sub>O<sub>3</sub> particles reaches or even exceeds 3 wt%, the nano-Sb<sub>2</sub>O<sub>3</sub> particles begin to agglomerate and form some larger agglomerates with increasing of the mass fraction of nano-Sb<sub>2</sub>O<sub>3</sub> particles due to the higher amount and surface energy of nano-Sb<sub>2</sub>O<sub>3</sub> particles. The agglomerates formation reduces the specific surface area of Sb<sub>2</sub>O<sub>3</sub> particles and also decreases the interfacial bonding strength between the particles and PP matrix, which makes the interfaces between Sb<sub>2</sub>O<sub>3</sub> aggregates and PP matrix to become some weaker points of nano-Sb<sub>2</sub>O<sub>3</sub>/BPS-PP composites. The agglomeration of nano-Sb<sub>2</sub>O<sub>3</sub> particles becomes more significant with increasing of the mass fraction of nano-Sb<sub>2</sub>O<sub>3</sub> particles. These interfacial weaker points not only reduce the crack growth resistance, but also become some new micro-crack sources. The forming and rapid propagating of these new cracks easily make the nano-Sb<sub>2</sub>O<sub>3</sub>/BPS-PP composites to fracture on macroscopic, resulting in decreasing of impact strength of the composites [13].

The SEM images of the nano-Sb<sub>2</sub>O<sub>3</sub>/BPS-PP composites containing modified and unmodified nano-Sb<sub>2</sub>O<sub>3</sub> particles with the mass fractions of 3 wt% are presented in Figure 6 (c) and Figure 6 (f), respectively. For Figure 6 (c), the modified nano-Sb<sub>2</sub>O<sub>3</sub> particles are uniformly wrapped in PP matrix, and the interfacial compatibility between the particles and PP matrix is better. In Figure 6 (f), nano-

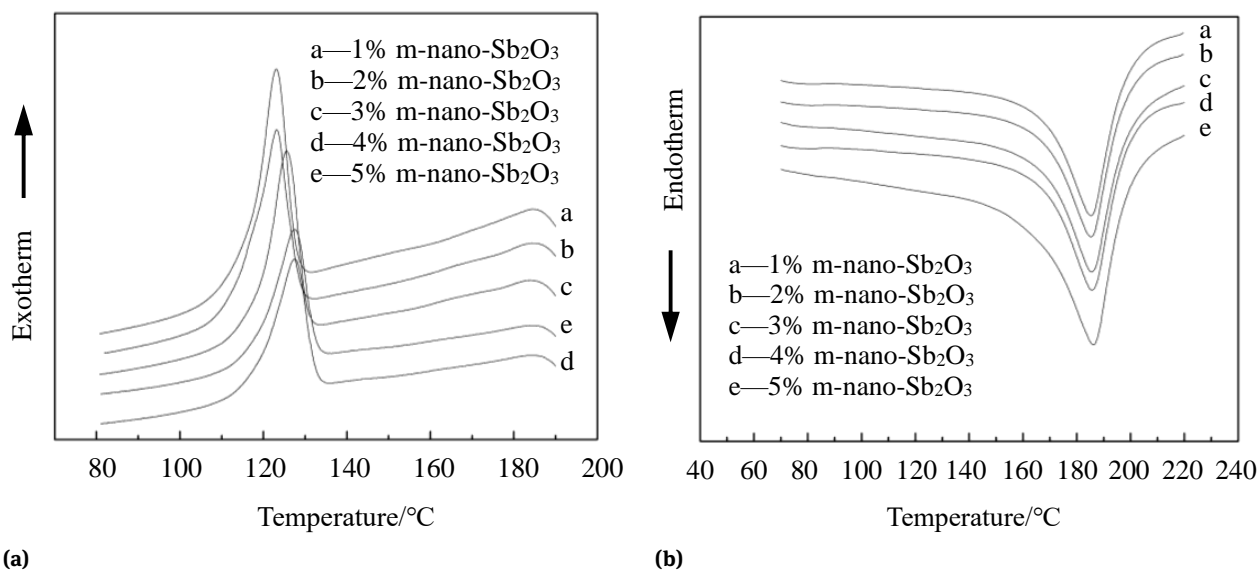


**Figure 7:** DSC crystallization curve and melting curve of the experimental nano-Sb<sub>2</sub>O<sub>3</sub>/BPS-PP composites (a) DSC crystallization curve; (b) DSC melting curve

Sb<sub>2</sub>O<sub>3</sub> particles form some large aggregates in PP matrix, and these aggregates drop off from PP matrix to form some micro-cracks. The interfacial compatibility between the Sb<sub>2</sub>O<sub>3</sub> aggregates and PP matrix is lower. There are some large peeling layers on the fracture surface, which belongs to a typical brittle fracture feature. It can decrease the impact strength of the nano-Sb<sub>2</sub>O<sub>3</sub>/BPS-PP composites significantly. It can be seen that the nano-Sb<sub>2</sub>O<sub>3</sub> particles modified by KH550 can not only improve the dispersion and interfacial compatibility between nano-Sb<sub>2</sub>O<sub>3</sub> particles and the PP matrix, but also improve the impact strength of nano-Sb<sub>2</sub>O<sub>3</sub>/BPS-PP composites.

### 3.3 Crystallinity of nano-Sb<sub>2</sub>O<sub>3</sub>/BPS-PP composites

Figure 7 shows the DSC crystallization curves and melting curves of the experimental nano-Sb<sub>2</sub>O<sub>3</sub>/BPS-PP composites containing modified nano-Sb<sub>2</sub>O<sub>3</sub> particles. It can be seen from Figure 7 that nano-Sb<sub>2</sub>O<sub>3</sub>/BPS-PP composites and PP both have a typical melting peak of  $\alpha$ -crystal of PP matrix. It indicates that the addition of the modified nano-Sb<sub>2</sub>O<sub>3</sub> particles doesn't affect the crystalline type of nano-Sb<sub>2</sub>O<sub>3</sub>/BPS-PP composites.

The non-isothermal crystallization parameters of nano-Sb<sub>2</sub>O<sub>3</sub>/BPS-PP composites with different mass fraction of nano-Sb<sub>2</sub>O<sub>3</sub> particles are shown in Table 3, in which  $T_m$  is the melting peak temperature,  $T_c$  is the crystallization peak temperature and  $X(t)$  is the crystallinity. Com-

pared with PP, the crystallization peak temperature and crystallinity of nano-Sb<sub>2</sub>O<sub>3</sub>/BPS-PP composites are higher than those of PP. When the mass fraction of nano-Sb<sub>2</sub>O<sub>3</sub> particles is 5 wt%,  $T_c$  of nano-Sb<sub>2</sub>O<sub>3</sub>/BPS-PP composites is 166.75°C and  $X(t)$  is 65.23%, which is 10.01°C and 46.16% higher than those of PP respectively. Nano-Sb<sub>2</sub>O<sub>3</sub> particles can improve the crystallinity and crystallization perfection of nano-Sb<sub>2</sub>O<sub>3</sub>/BPS-PP composites because it can promote the PP molecular chain to crystallize at a higher crystallization temperature increased by nano-Sb<sub>2</sub>O<sub>3</sub> particles. Nano-Sb<sub>2</sub>O<sub>3</sub> particles show the heterogeneous nucleation function in nano-Sb<sub>2</sub>O<sub>3</sub>/BPS-PP composites. The crystallinity of nano-Sb<sub>2</sub>O<sub>3</sub>/BPS-PP composites increases gradually with increasing of the mass fraction of nano-Sb<sub>2</sub>O<sub>3</sub> particles, but the increasing trend gradually slows down. This is due to the increasing of nucleation number in nano-Sb<sub>2</sub>O<sub>3</sub>/BPS-PP composites with increasing of the mass fraction of nano-Sb<sub>2</sub>O<sub>3</sub> particles, resulting in the in-

**Table 3:** Non-isothermal crystallization parameters of the experimental materials

Sample No.	$T_m/^\circ\text{C}$	$T_c/^\circ\text{C}$	$X(t)/\%$
1	120.36	156.74	44.63
2	123.95	163.63	53.42
3	123.19	164.30	60.32
4	124.34	167.21	62.79
5	124.63	167.25	64.83
6	124.64	166.75	65.23

creasing of the crystallinity. However, when the mass fraction of nano-Sb<sub>2</sub>O<sub>3</sub> particles exceeds 3 wt%, the amount and size of agglomerates of Sb<sub>2</sub>O<sub>3</sub> particles increase with increasing of mass fraction of nano-Sb<sub>2</sub>O<sub>3</sub> particles. These agglomerates reduce the number of effective nucleating particles, resulting in the increasing trend of crystallinity of nano-Sb<sub>2</sub>O<sub>3</sub>/BPS-PP composites slows down.

The crystallinity also effects on the mechanical properties of nano-Sb<sub>2</sub>O<sub>3</sub>/BPS-PP composites in some extent. The high crystallinity can make the grain of the composites more refining, the number of grains more increasing and the grain size distribution more uniform. The increasing of crystallinity and grain refinement can eliminate the stress concentration caused by the uneven grain distribution of nano-Sb<sub>2</sub>O<sub>3</sub>/BPS-PP composites under the external force, and improve the deformation resistance capacity of the composites [14]. Thus the mechanical properties of the nano-Sb<sub>2</sub>O<sub>3</sub>/BPS-PP composites can be effectively improved, namely the tensile strength and impact strength of the composites are improved. However, the improving toughness effect of the composites attributing to the improvement of interfacial interaction between nano-Sb<sub>2</sub>O<sub>3</sub> particles and PP matrix is stronger than that of the composites attributing to grain refinement of PP matrix caused by nano-Sb<sub>2</sub>O<sub>3</sub> particles [15]. When the mass fraction of nano-Sb<sub>2</sub>O<sub>3</sub> particles exceeds 3 wt%, the reducing effect of the mechanical properties attributing to aggregation of nano-Sb<sub>2</sub>O<sub>3</sub> particles is stronger than improving effect attributing to grain refinement caused by nano-Sb<sub>2</sub>O<sub>3</sub> particles in nano-Sb<sub>2</sub>O<sub>3</sub>/BPS-PP composites. Therefore, the mechanical properties of nano-Sb<sub>2</sub>O<sub>3</sub>/BPS-PP composites containing nano-Sb<sub>2</sub>O<sub>3</sub> particles with more than 3 wt% of the mass fraction show a downward trend.

## 4 Conclusions

Using Sb<sub>2</sub>O<sub>3</sub> nanoparticles (nano-Sb<sub>2</sub>O<sub>3</sub>) modified by silane coupling agent of KH550 as the additives, nano-Sb<sub>2</sub>O<sub>3</sub>/BPS-PP composites were prepared in the paper. The effects of nano-Sb<sub>2</sub>O<sub>3</sub> on the mechanical properties of nano-Sb<sub>2</sub>O<sub>3</sub>/BPS-PP composites were studied. The research obtained the following conclusions:

1. Silane coupling agent KH550 could effectively modify the surface of nano-Sb<sub>2</sub>O<sub>3</sub> particles, and then improve the dispersibility of the particles in nano-Sb<sub>2</sub>O<sub>3</sub>/BPS-PP composites and the interfacial compatibility between the particles and PP matrix.
2. The mechanical properties of nano-Sb<sub>2</sub>O<sub>3</sub>/BPS-PP composites were improved with increasing of the

mass fraction of nano-Sb<sub>2</sub>O<sub>3</sub> particles. When the mass fraction of nano-Sb<sub>2</sub>O<sub>3</sub> particles was 3 wt%, the tensile strength of nano-Sb<sub>2</sub>O<sub>3</sub>/BPS-PP composites was 43 MPa, which was 30.3% higher than that of PP. When the mass fraction of nano-Sb<sub>2</sub>O<sub>3</sub> particles was 2 wt%, the impact strength of nano-Sb<sub>2</sub>O<sub>3</sub>/BPS-PP composites was 44.19 kJ·m<sup>-2</sup>, which was 30.77% higher than that of PP.

3. The modified nano-Sb<sub>2</sub>O<sub>3</sub> particles could improve the crystallinity and grain refinement of nano-Sb<sub>2</sub>O<sub>3</sub>/BPS-PP composites, thus improve their mechanical properties.
4. There are two reasons for the improvement of the mechanical properties of nano-Sb<sub>2</sub>O<sub>3</sub>/BPS-PP composites with increasing of the mass fraction of nano-Sb<sub>2</sub>O<sub>3</sub> particles. On the one hand, the heterogeneous nucleation of nano-Sb<sub>2</sub>O<sub>3</sub> particles in PP matrix can refine grain and increase crystallinity of the composites. On the other hand, uniformly dispersed nano-Sb<sub>2</sub>O<sub>3</sub> particles can absorb part of the energy when the composites is subjected to external forces, and prevent micro-cracks propagating.

**Acknowledgement:** The work was supported by the National Natural Science Foundation of China (No. 51761025) and the Science and Technology Program Project Funds of Gansu Province of China (No. 17CX2JD075).

## References

- [1] Su F, Huang H, Zhou Y. Mechanical and thermal properties of PP/POE/Kaolinite ternary composites. *Polym. Mater. Sci. Eng.* 2009;25(10):94-97. Chinese.
- [2] Yan X, Xu X, Zhu T, Zhang C, Song N, Zhu L. Phase morphological evolution and rheological properties of polypropylene/ethylene octane copolymer blends. *Mat. Sci. Eng. A-Struct.* 2008, 476:120-125.
- [3] Maeng YJ, Yoon BS, Suh MH, Im WB, Lee SH. Effects of preferential encapsulation of glass fiber on the properties of ternary GF/PA/PP blend. *Polym. Composite. Polym. Composite.* 2000, 21(1):41-50.
- [4] Liu J, Zhang L, Yang H, Ding X, Chen Q, Lu Y. Numerical investigation of the thermal property of particle filled polymer matrix composite. *Acta Mater. Compos. Sin.* 2009,26 (1): 36-42. Chinese.
- [5] Yang W, Xu J, Niu L, Kang C, Ma B. Effects of high energy ball milling on mechanical and interfacial properties of PBT/nano-Sb<sub>2</sub>O<sub>3</sub> composites. *J. Adhes. Sci. Technol.* 2018,32 (3): 291-301.
- [6] Rong MZ, Zhang MQ, Zheng YX, Zeng HM, Friedrich K. Improvement of tensile properties of nano-SiO<sub>2</sub>/PP composites in relation to percolation mechanism. *Polym.* 2001,42 (7): 3301-3304.
- [7] Laachachi A, Cochez M, Ferriol M, Leroy E, Lopez Cuesta JM, Ogeta N. Influence of Sb<sub>2</sub>O<sub>3</sub> particles as filler on the thermal stabil-



- ity and flammability properties of poly (methyl methacrylate) (PMMA). *Polym. Degrad. Stabil.* 2004, 85(1): 641-646.
- [8] Xu J, Liu X, Yang W, Niu L, Zhao J. Flame Retardant Performance of Nano-Sb<sub>2</sub>O<sub>3</sub>/BEO/PP Composites. *J. Mater. Eng.* 2019, 47(1): 84-90. Chinese.
- [9] Xu J, Zhao J, Niu L, Yang W, Liu X, Kang C, Ma B. Mechanical properties of polypropylene matrix composites strengthened by nano Sb<sub>2</sub>O<sub>3</sub>. *Acta Mater. Compos. Sin.* 2018, 35(9): 2465-2472. Chinese.
- [10] Liu X, Chen X, Ren J, Zhang C. TiO<sub>2</sub>-KH550 nanoparticle-reinforced PVA/xylan composite films with multifunctional properties. *Materials*. 2018, 11(9): 1589.
- [11] Blake R, Gun'ko YK, Coleman J, Cadek M, Fonseca A, Nagy JB, et al. A generic organometallic approach toward ultra- strong carbon nanotube polymer composites. *J. Am. Chem. Soc.* 2004, 126(33): 10226-10227.
- [12] Zheng Y, Cai C, Shen Z, Ma S, Xing Y. Toughening and strengthening of micro-an nano-SiO<sub>2</sub>/PP composite. *Acta Mater. Compos. Sin.* 2007, 24(6): 19-25. Chinese.
- [13] Xu XM, Zhang YD, Li BJ, Lu HM, Zhang ZJ. The Interface structure of PA66/SiO<sub>2</sub> nanocomposites and its effect on mechanical Properties. *Polym. Mater. Sci. Eng.* 2009, 25(2): 41-44. Chinese.
- [14] Xiong F, Xiao Z, Lu D, Guan R. Influence of  $\alpha$ -Nucleating agent on PP crystallinity and morphology. *Mod. Plast. Process. Appl.* 2006(1):39-42. Chinese.
- [15] Liu J, Hu F, Yu Q. Nucleation and crystallization and mechanical properties of nano-ZnO/ polypropylene composites modified by maleic anhydride grafted polypropylene. *Acta Mater. Compos. Sin.* 2017, 34(7): 1526-1532. Chinese.